Towards ultrahigh-contrast ultraintense laser pulses—complete characterization of a double plasma-mirror pulse cleaner

T. Wittmann[a)]
Laboratoire pour l'Utilisation des Lasers Intenses (LULI), Ecole Polytechnique Route de Saclay, F91128 Palaiseau, France and Department of Optics and Quantum Electronics, University of Szeged Dóm square 9, H6720 Szeged, Hungary

J. P. Geindre and P. Audebert
Laboratoire pour l'Utilisation des Lasers Intenses (LULI), Ecole Polytechnique Route de Saclay, F91128 Palaiseau, France

R. S. Marjoribanks
Department of Physics, and Institute for Optical Sciences, University of Toronto, 60 St. George Street, Toronto, Ontario M5S 1A7, Canada

J. P. Rousseau, F. Burgy, D. Douillet, T. Lefrou, K. Ta Phuoc, and J. P. Chambaret
Laboratoire d'Optique Appliquée (LOA), ENSTA - Ecole Polytechnique, Chemin de la Hunière, F91761 Palaiseau, France

(Received 8 December 2005; accepted 27 June 2006; published online 25 August 2006)

The effects of small amounts of energy delivered at times before the peak intensity of ultrahigh-intensity ultrafast-laser pulses have been a major obstacle to the goal of studying the interaction of ultraintense light with solids for more than two decades now. We describe implementation of a practical double-plasma-mirror pulse cleaner, built into a $f=10$ m null telescope and added as a standard beamline feature of a 100 TW laser system for ultraintense laser-matter interaction. Our measurements allow us to infer a pulse-height contrast of 5×10^{11}—the highest contrast generated to date—while preserving ~50% of the laser intensity and maintaining excellent focusability of the delivered beam. We present a complete optical characterization, comparing empirical results and numerical modeling of a double-plasma-mirror system. © *2006 American Institute of Physics.* [DOI: 10.1063/1.2234850]

I. INTRODUCTION

Owing to the rapid advances in high-intensity short-pulse laser technology, available peak intensities of laser pulses have increased by more than three orders of magnitude over the past decade, approaching 10^{22} W/cm^2 at the laser focus.[1,2] Such extremely high intensities are expected to open a route to the exploration of entirely new phenomena in laser-matter interaction. The principal barrier that has so far blocked this route is the nonideal temporal profile of the optical pulses. As peak laser powers have jumped by orders of magnitude, techniques of pulse manipulation have not kept pace; consequently, along with the main pulses, prepulse energies have also been amplified until they themselves initiate optical breakdown and other nonlinearities. Limited by the imperfections of chirped pulse amplification and pulse compression (CPA) laser techniques, current prepulse intensity contrasts are typically 10^6–10^7 of peak on a time scale of nanoseconds, and 10^4 of peak on a picosecond time scale.

As a result of significant fluence delivered in the pulse-pedestal common in CPA recompression, and in prepulses that may arise from pulse-selection imperfections, a preformed plasma may evolve from the target. This preplasma expands to low densities, 1–100 μm from the target surface. In place of a steep density gradient at the surface of a solid target, the main pulse interacts with the low density preplasma, which decouples energy deposition from the solid and which considerably increases the complexity of the interaction. At very high intensities, even a perfectly clean temporally Gaussian pulse will lead to movement of a plasma critical-density surface before the maximum intensity. Although laser intensities sufficient to demonstrate qualitatively new physics have now been available for some time, experiments specifically to access laser-solid interactions, e.g., in high-order harmonic generation or particle acceleration, have remained tantalizingly elusive. Therefore, in this field in recent years, increasing pulse contrast and steepening the leading edge of these ultraintense laser pulses has become a broadly held goal of primary importance.

In order to provide a solid target surface for the main pulse, in ultraintense laser-matter interaction, the pedestal should be kept below the optical damage threshold of the target material. For metals such as aluminum, and subpicosecond pulses, this corresponds to an intensity below 10^{11} W/cm^2, though for longer prepulses the integrated fluence may be more significant. To maximize this threshold, and minimize the impact of laser pre-pulses, glasses, crystals

[a)]Author to whom correspondence should be addressed; current address: Max-Planck-Institut für Quantenoptik Hans-Kopfermann-Strasse 1, D-85748 Garching, Germany; electronic mail: wittmann@greco2.polytechnique.fr

and other materials with very small linear absorption at typical laser wavelengths have been used in experiments. For example, barium borosilicate glass has been reported a threshold fluence for picosecond pulses at 780 nm of 2.2 ± 0.3 J/cm^2 for Ref. 3; in a similar study, fused silica has been characterized with a damage threshold of $\sim$1.3 J/cm^2 (526 nm) and $\sim$2.6 J/cm^2 (1053 nm).[4] These results are consistent with our earlier study[5] on plasma mirrors, in which we have reported 5 J/cm^2 threshold fluence for reflective plasma formation in the 60 fs–4 ps range using 780 nm *s*-polarized laser light.

Therefore, laser pulses approaching 10^{22} W/cm^2 intensity at the target focus will require a temporal contrast of at least 10^{10}. Such a high ratio is beyond the intrinsic contrast of currently running CPA systems—and an evolvable solution is necessary, ever increasing the contrast to limit the prepulse intensity, as higher peak-power systems emerge. Although there has been intensive research, comprising mostly laser techniques as such Refs. 6–9, no method has been found so far which can meet the necessarily high requirements.

The "plasma mirror" (PM) concept—a self-induced ultrafast optical shutter—appears to be a promising solution to this problem. Its operation is based on the effect of ultrafast ionization by high-intensity laser light. The laser pulse strikes a flat, optically transparent target. If the fluence of the pulse is optimal, the leading pedestal and prepulses freely traverse the target, but the leading edge of the main pulse ionizes it, triggering a dense, highly reflective plasma layer. This plasma mirror reflects the main pulse. Within the optimum fluence range, and for femtosecond pulses, the hydrodynamic expansion of the plasma layer is negligible compared to a wavelength during the main pulse,[5] thus the reflection from the PM remains specular, and almost no degradation of the reflected beam results. The contrast is improved by a factor equal to the ratio of the reflectivity of the PM and that of the original cold substrate.

Recognition of the impact of preplasmas in various laser-matter interaction experiments led to the technique of plasma-mirror pulse cleaners, and their preliminary characterization. An early experiment demonstrated the performance of the technique in the generation of x-ray emitting solid-density plasmas.[10] Most studies have concentrated on the measurement of reflectivity as a function of laser intensity.[11–14] Some have complemented this with the measurement of contrast improvement.[12,13] The *de facto* effect of spatial filtering, an important additional feature of the PM, was also investigated:[14] placing the PM at the laser focus, intense spatial structures decompose, in the Fourier plane on the PM, into high spatial frequencies at moderate intensities. These are weakly reflected, and where the local intensity peaks exceed threshold the energy is diffracted into a large angle.

Of central importance, time resolved investigations have proved that the change in reflectivity is instantaneous compared to the applied pulse width, even at intensities near threshold;[15–17] this fast transition permits the suppression of a pulse pedestal while not "softening" the leading edge of or losing significant energy from the intense ultrafast pulse.

We have previously conducted a complete theoretical and experimental study of an *ad hoc* double-plasma mirror (DPM) installed in the final beam-path approaching focus.[5] Based on these results, a single plasma-mirror (PM) system was incorporated into a 10 TW laser.[18] In this, an optical flat, antireflection coated for an *s*-polarized beam, served as a PM which increased the contrast ratio routinely by a factor of 200. Its effectiveness was demonstrated by the generation of spectrally clean high-order harmonics in a steep density gradient on a solid target.

Such an improvement with a single PM system is satisfactory for TW-class lasers, but for state-of-the art ultraintense lasers further improvement is necessary. Inserting multiple plasma mirrors into the system is a potential solution: contrast enhancement of 10^3-10^4 can be achieved by cascading two PMs.[19] The development and complete characterization of such a cascaded double PM system is the subject of this article.

This system, engineered as a standard system feature and easily added or bypassed with a single kinematic stage, has been installed in the 100 TW "Salle jaune" Ti:sapphire laser of the Laboratoire d'Optique Appliquée, ENSTA and Ecole Polytechnique, improving its intrinsic contrast to a final ratio of 10^{11}. Our detailed characterization includes measurement and simulation of plasma reflectivity and propagated beam quality, as transported from the DPM to the final focus; good agreement is obtained between theory and empirical results.

II. EXPERIMENTAL SETUP

The 100 TW Salle jaune laser delivers 25 fs pulses of energies up to 2.5 J at 780 nm wavelength, with up to 10 Hz repetition rate.[20] The peak-to-background contrast of the laser, according to third-order autocorrelation measurements, slightly exceeds 10^7 on a nanosecond time scale; it is 10^4 on the picosecond time scale. This contrast was checked regularly during the experiment and no appreciable fluctuation was observed.

An important consideration in the design of the DPM system was that the PMs should be easily added into, and removed from, the beam path on a shot-to-shot basis. A mirror-slide switchyard accomplished this, with the DPM system installed in a cross tube of the main vacuum beamline. The double plasma mirror scheme was introduced (Fig. 1) in the middle of a folded, 10 m focal length, null telescope, which creates an intermediate focus for the laser beam, subsequently recollimating it to continue on to the interaction chambers. At this intermediate focus the two PMs are situated, both with a 45° angle of incidence. Fluence on the PMs is varied by altering beam parameters upstream, using a deformable mirror. The beam introduced to the null telescope has a diameter of 5.5 cm; at the plasma mirrors, the intermediate focus is *s* polarized. Both PMs were quartz plates, 10 cm$\times$10 cm, antireflection coated to minimize intrinsic reflectivity (0.3%).

The contrast improvement factor is essentially the ratio between the reflectivity of the plasma mirror and this intrinsic reflectivity of the "cold" mirror. Computer-controlled stages translate the PMs parallel to their surface, to provide a

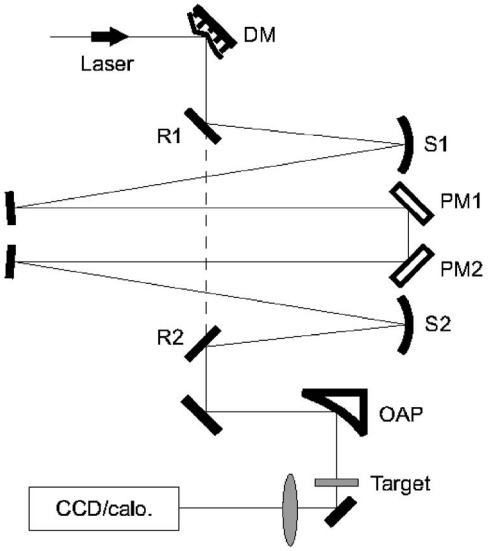

FIG. 1. Experimental setup of the double PM system. An $f=10$ m null telescope (spherical mirrors S1 and S2) creates an intermediate focus for the laser beam and then recollimates it; near this focus, the plasma mirrors (PM1 and PM2) are situated, both with a 45° angle of incidence. The fluence on the PMs was varied by changing the radius of curvature of the deformable mirror (DM). Mirrors R1 and R2 on a kinematic slide permit the DPM to be inserted (solid line) or bypassed (dashed line). Final focus was created by an off-axis-parabolic mirror (OAP), and monitored by a CCD and a calorimeter.

fresh surface for each shot—several thousand shots are possible before replacement of the mirrors is required. The two plates were positioned at right angles to each other (Fig. 1), separated by 14 cm as measured along the beam path. It was found by preliminary calculations that by setting this distance the fluence would be ~six times higher on the second PM. By taking into account the contrast enhancement factor of the first mirror, it was ensured that the second PM would subsequently operate without the risk of preplasma formation. The higher fluence on the second mirror then yields a larger reflectivity.

The highest reflectivity and best beam profile were optimized as a function of the incident fluence on the PMs. For this, the fluence was scanned by changing the radius of curvature of the deformable mirror (BIM36, Cilas), whose standard function in the laser is the correction of the spatial phase front. We were able to change the position of the null telescope's focal spot over a range of 80 cm, changing the fluence simultaneously on both PMs.

The fluence on each PM was monitored using ordinary web cameras (360 USB 2.0 Spacec@m, TRUST), (Fig. 2).

The most important parameter of the optimization, the reflectivity of the system, was detected by measuring the laser energy incident on and reflected through the DPM system. Each was measured with a calorimeter placed in the target chamber, first bypassing the DPM and then deploying it. The incident energy at the first PM, combined with the laser spot image there, yielded the incident fluence.

The final focus at the experiment target also was imaged, using a 16 bit charge coupled device (CCD) camera (Andor), and like other parameters it was recorded while varying fluence conditions. Small displacements of the position of the final focus beam waist, caused by the varying divergence of the beam during optimization with the deformable mirror, were compensated for by moving the imaging CCD.

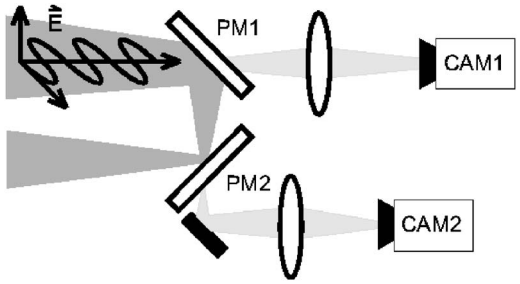

FIG. 2. Schematic of fluence measurement on PMs: *s*-polarized beam reflects from PM1 and then PM2. The laser spots on both PMs were imaged onto web cameras (CAM1 and CAM2).

III. CHARACTERIZING DPM REFLECTIVITY

Figure 3 shows the time- and space-integrated reflectivity (overall efficiency), and the time-integrated reflectivity measured at the center of the final target focus (spatial peak reflectivity) as a function of the plasma-mirror focal position. The same reflectivity curves obtained from the theoretical modeling are also depicted. The position of the focus is determined with respect to the PMs: the zero of the axis corresponds to the focal spot positioned on the second PM. For values less than zero, the focus approaches the first PM; −14 cm corresponds to focusing onto the first plasma mirror. For values greater than zero, the focus shifts behind the second PM. As can be readily seen, the optimal position with the highest reflectivity—31% overall and 47%–57% peak reflectivity—is at the zero position, as anticipated in the design. At this position the first PM is subject to a peak fluence of 200 J/cm^2 while the second PM sees 800 J/cm^2. For these fluences, and making use of our earlier single PM

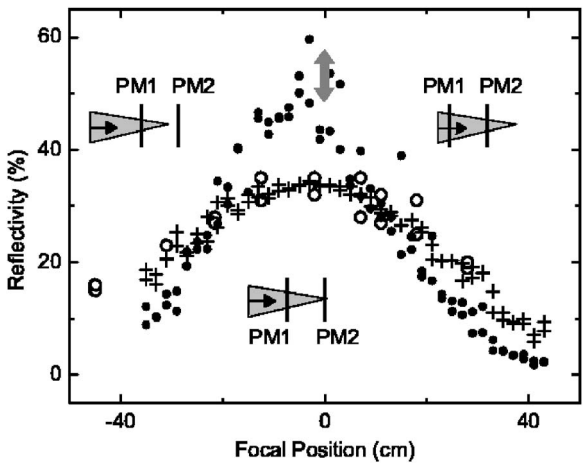

FIG. 3. Spatial peak and overall reflectivity of the DPM system versus focal position. Spatial peak reflectivity: experimental result at the maximum reflectivity position (gray arrow), and numerical results over the whole range (solid circles). Overall reflectivity: experimental (open circles) and numerical results (crosses). The position of the focus is referenced with respect to the PMs: the zero of the axis corresponds to the focal spot positioned on the second PM. The random phase perturbation was different for each run of the simulation, producing the scatter observed in the numerical data sets.

model,[5] the corresponding peak reflectivities are predicted to be 70% and ~80%. Together with the low-intensity reflectivity known for the antireflection coatings, these reflectivities lead to contrast enhancements of ~200 overall, and ~250 peak, for each plasma mirror in succession.

Examining the reflectivity curves further, moving in either direction away from the ideal zero position shows a decrease in both overall and peak reflectivity, and consequently in contrast improvement. This decrease indicates that at the zero position both PMs were optimally positioned to operate at the ideal fluence regime, i.e., where the pedestal is just below the breakdown threshold. Higher fluence on either mirror will lead to too-early triggering of the plasma layer, while a lower fluence will unnecessarily reduce plasma reflectivity. In summary, the DPM system is understood to improve the contrast by a factor of 5×10^4 with a decrease of peak intensity, at the center of the focal spot, of ~50%.

IV. MODELING OPTICAL TRANSPORT FROM THE DOUBLE PLASMA MIRROR

The computer simulation developed to model the DPM in operation is a simple paraxial diffraction/propagation model coupled with the results of plasma modeling of the spatial reflectivity of the PMs, found from our earlier "population propagation" model.[5] We calculate the optical field on each element up to the final focus; the steep fluence dependence of the PM reflectivity R is phenomenologically approximated by a step-like response $R=75\%$ above 6 J/cm^2 and $R=0$ below it. The fluctuation of the spatial uniformity in the experimental beam quality was taken into account in our modeling by adding 0.7 wave rms random phase disturbance to the optical field. This random phase perturbation was different for each run of the simulation, producing the scatter observed in the data sets presented here. As has already been shown in Fig. 3, the peak and overall reflectivity curves obtained from the model agree well with the experimental results.

A key aspect of any optical system is its impact on focusability. We have performed an extensive characterization of the beam quality after the DPM. This included parallel experimental measurements and computer modeling of the development of the fluence distribution in propagation through the whole setup: intermediate-field calculations and fluence-distribution measurements at each PM, and the far-field fluence distribution at the final focus. Figure 4 shows the beam profiles on the PMs at low flux, both measured and modeled, using the maximum-reflectivity focusing. The beam diameter on the first PM is ~1.2 mm with an average fluence of 200 J/cm^2 and as it can be readily seen the profile is strongly modulated in intensity, which is a potentially significant drawback of placing the first PM in the intermediate field of the beam. This rough profile leads to spatial variations in PM reflectivity, imparting further amplitude distortions. However, in our earlier report,[5] in good agreement with the recent results of Dromey *et al.*,[21] we found that these distortions are weak and do not significantly impair the focusability. The focus on the second PM is circular with a smooth profile. The diameter of the focus is ~200 μm and the average fluence is 800 J/cm^2.

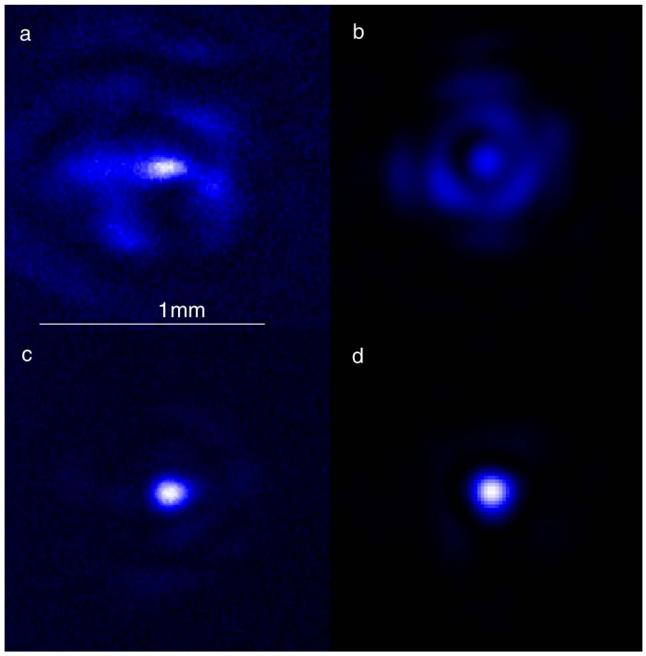

FIG. 4. Beam profiles on PM plates: (a) experimental observation and (b) numerical simulation of the fluence distribution on PM1; (c) experimental observation and (d) numerical simulation of the fluence distribution on PM2.

Figure 5 depicts the final focal spot at the target plane, recorded by the 16 bit CCD camera, with and without the DPM system. It is evident from these images that the quality of the focus with the DPM in place is at least as good as without. The sizes of the foci are practically the same, and no degradation in the beam profile can be observed. The only noticeable difference is that the energy in the foot around the focal spot is decreased significantly by the DPM. This is because the second PM was operating in the beam's far field, and acted as a spatial filter. This effect can also be clearly seen in the images produced by the numerical simulation.

This result is also presented in Fig. 6, where we have normalized the different focal spots to the peak intensity and measured the energy encircled within different radii. From

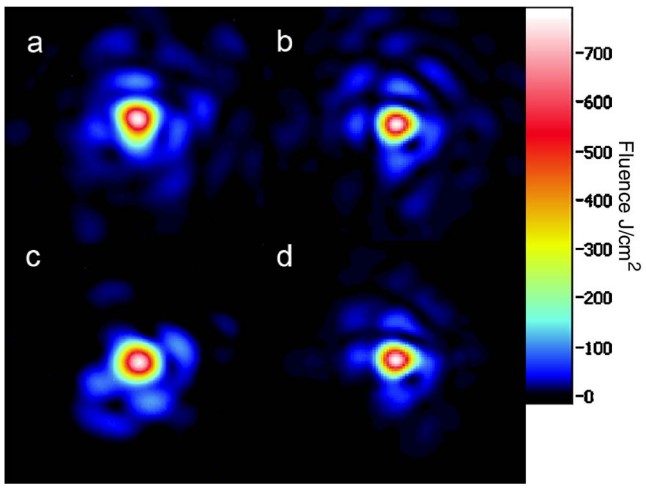

FIG. 5. Focal spots in final target plane without and with the DPM system: (a) experimental observation and (b) numerical simulation of the final focus without the DPM system; (c) and (d) experimental and numerical results obtained for the final focus with the DPM system.

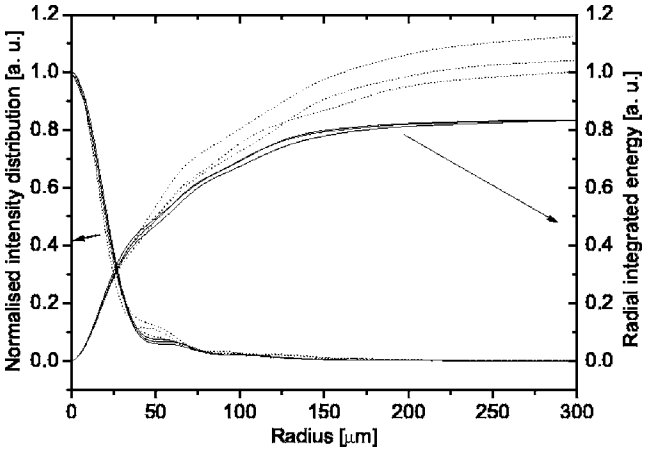

FIG. 6. Normalized intensity distribution for three experimental shots with plasma mirror and three experimental shots without plasma mirror (left side of graph) and corresponding radial integrated energy (right side of graph) for the six shots. Dashed line: without DPM; solid line: with DPM. The addition of the DPM reduces the energy deposited outside the focal spot, as compared to the case without DPM.

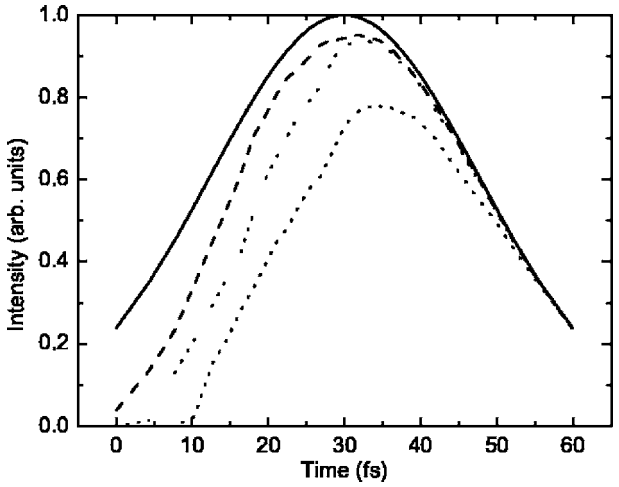

FIG. 8. Front-edge steepening of the reflected pulse at different pulse energies. The original pulse shape (solid line) is compared to reflected pulses on the assumption of incident pulse energies of 1 J (dashed line), 0.5 J (dot-dashed line) and 0.25 J (dotted line).

the curve we can see that the DPM changes the balance of energy at the focal peak, relative to the wings of the focal spot: the energy lost, with the use of plasma mirrors, is disproportionately from the outside of the focal spot, while tending to preserve the peak.

For a more comprehensive characterization of the beam characteristics after the DPM, an imaged z scan was made around the final focus and the change in peak intensity was investigated. In Fig. 7, the peak fluence with and without the DPM is plotted against the displacement of the object plane from the focal spot position. Moving with displacement z out of the focal plane, the peak fluence of the beam with the DPM drops from its maximum value much the same as does the peak fluence without the DPM. This implies that the DPM does not have a strong effect on the laser intermediate field.

In addition to improving the contrast and the intensity profile of the laser pulse, there is an additional significant improvement conferred by the DPM system: control of the focused fluence at the second plasma mirror permits the threshold for mirror formation to be set at a point within the leading edge of the pulse—which will steepen the rising edge of the pulse. This leading-edge steepening is highly advantageous to the creation of near-solid-density short-scale-length plasmas. Experimental confirmation of this effect, on a few-femtosecond time scale, lays beyond the scope of the current investigation, but we have performed model calculations to characterize the temporal changes of the pulse. These simulations were based on our earlier population propagation model.[5]. Figure 8 shows the leading-edge steepening, compared to the original pulse, for different pulse energies. The steepest rising edge can be achieved in our system with pulse energies between 0.5 and 1 J, in good agreement with our heuristic expectations: this energy leads to a fluence insufficient to trigger reflective-plasma formation until the leading edge of the main pulse itself arrives, but high enough to ensure that the reflectivity at the temporal peak exceeds 90%.

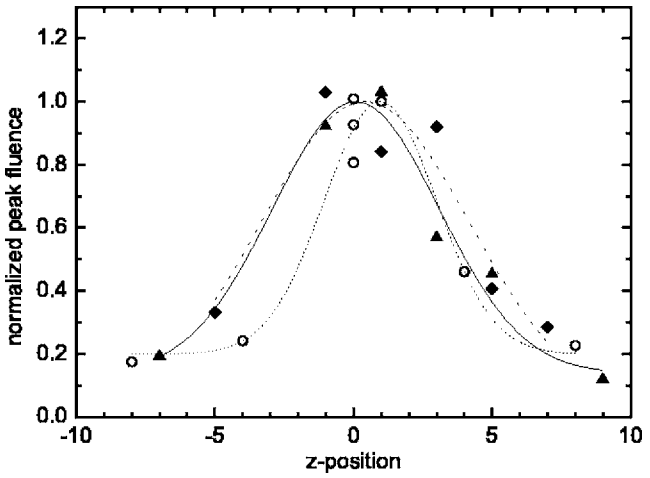

FIG. 7. Empirical spatial-peak fluence as a function of position around best focus: beam z scan without (triangle and solid line, diamond and dashed line) and with (open circles, dotted) DPMs. For ease of comparison, all curves are normalized to unity. The lines are provided as a guide to the eye.

V. DISCUSSION AND OUTLOOK

In summary, we demonstrate a double plasma-mirror system for pulse-contrast enhancement, which has more than 50% efficiency in intensity and highly repeatable in its characteristics. It has been engineered as a standard system feature and is easily added or bypassed with a single kinematic stage in a 100 TW Ti:sapphire research laser. It provides minimal phase disturbance, preserving final beam focusability and on-target intensity. The pulse contrast—inferred from hot and cold reflectivities of the plasma mirrors—is enhanced by 5×10^4, for a final contrast better than 10^{11}; to the best of our knowledge these are the highest-contrast pulses produced to date. Of equal importance, it is an engineered system which now provides a standard optional system feature for regular use.

Our detailed characterization includes measurement and simulation of plasma reflectivity and propagated beam qual-

ity, from the DPM to the final focus. The experimental findings are in very good agreement with the model calculations. The most important feature of the DPM is that no degradation in beam quality or focusability has been observed, but the contrary: a slight improvement of the profile in the final focus has been shown, due to the spatial filtering effect of the second PM. We conclude that a critical point of any multiple-PM system in the future will be the first mirror that should operate in the near or intermediate field. As we demonstrate conclusively, this results in no loss of beam quality. The obtained focal spots are repeatable—no appreciable fluctuation from shot to shot was perceived.

These outstanding features will make multiple-plasma-mirror systems an integral part of high intensity lasers and soon the generation of temporally clean ultraintense laser pulses will be commonplace. We believe that using our model as a fundamental base it has become feasible to design and attach DPM systems to any ultrafast laser operating above the terawatt level. Many areas of current research—in particular the generation of relatively intense x-ray pulses by high-order harmonic generation on solid targets, which is of key importance—have been strongly hindered so far by the presence of prepulses and leading pedestal. Now, cascaded PM systems are in a position to be the solution to this problem. The high-contrast pulses provided by these devices are expected to open up new prospects in high intensity laser-matter interaction experiments. Due to the continual increase in the peak power of the lasers, further contrast enhancement will be necessary in the future; a third PM inserted close to the focus, like the second one here, would provide a practical solution.

[1] J. D. Bonlie, F. Patterson, D. Price, B. White, and P. Springer, Appl. Phys. B **70**, S155 (2000).
[2] S.-W. Bahk, P. Rousseau, T. A. Planchon, V. Chvykov, G. Kalintchenko, A. Maksimchuk, G. A. Mourou, and V. Yanovsky, Opt. Lett. **29**, 2837 (2004).
[3] W. Kautek, J. Krüger, M. Lenzner, S. Sartania, Ch. Spielmann, and F. Krausz, Appl. Phys. Lett. **69**, 3146 (1996).
[4] B. C. Stuart, M. D. Feit, A. M. Rubenchik, B. W. Shore, and M. D. Perry, Phys. Rev. Lett. **74**, 2248 (1995).
[5] G. Doumy, F. Quéré, O. Gobert, M. Perdix, Ph. Martin, P. Audebert, J. C. Gauthier, J. P. Geindre, and T. Wittmann, Phys. Rev. E **69**, 026402 (2004).
[6] M. Nantel, J. Itatani, A.-C. Tien, J. Faure, D. Kaplan, M. Bouvier, T. Buma, P. A. VanRompay, J. Nees, P. P. Pronko, D. Umstadter, and G. Mourou, IEEE J. Quantum Electron. **4**, 449 (1998).
[7] J. Itatani, J. Faure, M. Nantel, G. Mourou, and S. Watanabe, Opt. Commun. **148**, 70 (1998).
[8] G. Chériaux *et al.*, Conference on Lasers and Electro-Optics, Postconference Technical Digest, 2001, p. 45.
[9] I. Jovanovic, B. J. Comaskey, C. A. Ebbers, R. A. Bonner, D. M. Pennington, and E. C. Morse, Appl. Opt. **41**, 2923 (2002).
[10] H. C. Kapteyn, M. M. Murnane, A. Szoke, and R. W. Falcone, Opt. Lett. **16**, 490 (1991).
[11] Ch. Ziener, P. S. Foster, E. J. Divall, C. J. Hooker, M. H. R. Hutchinson, A. J. Langley, and D. Neely, J. Appl. Phys. **93**, 768 (2003).
[12] S. Backus, H. C. Kapteyn, M. M. Murnane, D. M. Gold, H. Nathel, and W. White, Opt. Lett. **18**, 134 (1993).
[13] D. M. Gold, Opt. Lett. **19**, 2006 (1994).
[14] D. M. Gold, H. Nathel, P. R. Bolton, W. E. White, and L. D. Van Woerkom, SPIE Short Pulse High Intensity Lasers and Applications **1413**, 41 (1991).
[15] Z. Bor, B. Rácz, G. Szabó, D. Xenakis, C. Kalpouzos, and C. Fotakis, Appl. Phys. A **60**, 365 (1995).
[16] B. Hopp, Z. Tóth, K. Gál, Á. Mechler, Zs. Bor, S. D. Moustaizis, S. Georgiou, and C. Fotakis, Appl. Phys. A **69**, S191 (1999).
[17] Z. Tóth, B. Hopp, Á. Mechler, Zs. Bor, S. D. Moustaizis, A. Athanassiou, S. Georgiou, C. Kalpouzos, and C. Fotakis, Laser Phys. **10**, 241 (2000).
[18] P. Monot, G. Doumy, S. Dobosz, M. Perdix, P. D'Oliveira, F. Quéré, F. Réau, Ph. Martin, P. Audebert, J. C. Gauthier, and J. P. Geindre, Opt. Lett. **29**, 893 (2004).
[19] I. Watts, M. Zepf, E. L. Clark, M. Tatarakis, K. Krushelnick, A. E. Dangor, R. M. Allott, R. J. Clarke, D. Neely, and P. A. Norreys, Central Laser Facility, Rutherford Appleton Laboratory (RBL) Annual Report 2000/2001, p. 32.
[20] M. Pittman, S. Ferré, J. P. Rousseau, L. Notebaert, J. P. Chambaret, and G. Chériaux, Appl. Phys. B **74**, 529 (2002).
[21] B. Dromey, S. Kar, M. Zepf, and P. Foster, Rev. Sci. Instrum. **75**, 645 (2004).